Influence of Agarose Gel on Electrophoretic Stretch, on Trapping, and on Relaxation of DNA

Dirk Stigter†

Department of Pharmaceutical Chemistry, University of California, San Francisco, California 94143

Received May 30, 2000; Revised Manuscript Received September 5, 2000

ABSTRACT: The long-range hydrodynamic interaction between DNA and agarose gel is treated by modeling the gel as a uniformly porous medium, characterized by Debye's hydrodynamic shielding length L. We derive the liquid flow field around a solid sphere moving through the gel and the hydrodynamic friction of the sphere. These results are used in the hydrodynamic interaction between DNA and the gel during electrophoretic stretch and relaxation of stretched DNA. Experiments by Gurrieri, Smith, and Bustamante (*Proc. Natl. Acad. Sci. USA* **1999**, *96*, 453) lead to an estimate of $L = 4 \times 10^{-8}$ m for the shielding length of 1.2% agarose gel. The critical trapping force in such a gel is found to be 29 pN, consistent with results reported by Gurrieri et al. (1999). If the unwinding of the double helix at the gel contact is essential for trapping, addition of salt should cause a significant increase in the critical field strength for trapping DNA. Relaxation of the length and of the tether force of initially stretched DNA is described by a balance between the elastic forces (tension gradients) of DNA and hydrodynamic friction. Brownian motion is introduced in an approximate way. Its effect on the relaxation is moderate. The influence on relaxation of several factors, including gel porosity and DNA size, is studied. The scaling with DNA size is better for relaxation of the tether force than of the DNA extension. The relaxation of DNA predicted in pure solvent agrees fairly well with experiments by Perkins, Quake, Smith, and Chu (*Science* **1994**, *264*, 822).

1. Introduction

Gel electrophoresis for the size fractionation of DNA is well understood in a qualitative way. This paper addresses two outstanding issues for a quantitative theory, the hydrodynamic properties of the gel and the relaxation of stretched DNA. The difference between the apparent mobility of DNA during gel electrophoresis and its mobility in free solution[1] is a measure of the interaction of DNA with the gel. Very helpful for a qualitative understanding have been microscopic observations of the dynamics of single DNA molecules stained with a fluorescent dye.[2−4] These studies show that the progress of DNA through the gel occurs in cycles, somewhat similar to the motion of a caterpillar. The observed cyclic changes of DNA conformation, however, do not shed light on the friction between DNA and the gel. The exact nature of this friction is an unresolved issue.

Short-range solid (contact) friction, short-range liquid (lubricated) friction, and long-range hydrodynamic perturbations suggest themselves as possible modes of interaction between DNA and gel fibers. Burlatsky and Deutch[5] have considered solid friction as a main factor in the apparent mobility of DNA. On the other hand, Viovy and Duke[6] propose that, in general, Brownian motion might lead to less contact between entangled chain segments and the gel and, hence, to a smaller effect of solid friction. During gel electrophoresis Song and Maestre[3] observed DNA chains hooked around gel fibers in a U-shape, a prominent conformation of DNA on its way through the gel. They measured the velocity of the DNA sliding toward the long leg of the U, and calculated the friction coefficient with the gel fiber at the pivot point.

† Correspondence address: 1925 Marin Ave, Berkeley, CA 94707.

Short range sliding friction is not the only interaction between DNA and a gel, as shown convincingly in experiments by Gurrieri et al.[4] These authors have compared tether forces on a dimer of λ-DNA (97 kbp) stretched electrophoretically in a gel with 1.2% agarose and in pure solvent. They report that the presence of the gel increases the tether force 4-fold. In these experiments, we do not have sliding friction with the gel because the DNA is tethered at one end and, hence, is stationary in the applied field. But we do have a difference in long-range hydrodynamic interaction due to the forces of the gel on the liquid. In a recent treatment of electrophoretic stretch in free solution, Stigter and Bustamante[7] showed that, although the DNA itself is stationary, there is around the stretched chain a long-range flow field, due to the net electric force on the small ion atmosphere around the DNA. This flow field may be obstructed by the gel.

It has been known for a long time that in free solution the hydrodynamic perturbations around a particle during electrophoresis and during sedimentation are very different, short range in the former, but long range in the latter case.[8] In gel electrophoresis, we have a combination of short-range and long-range perturbations, depending on what part of the dynamic cycle is considered. In this paper, we study the long-range perturbations by the gel. The treatment of the gel, as a fluid medium of continuous and uniform porosity, is similar to that of a polymer coil by Debye and Bueche.[9] As is usual in polymer hydrodynamics, we represent segments of the DNA chain by equivalent spheres. This reduces DNA hydrodynamics to the friction of such spheres and the pair interaction between them. The next section deals with the motion of a solid sphere through a gel. In section 3, the treatment developed for stretching DNA in free solution[7] is extended to electrophoretic stretch in agarose gels. Here we also investigate

10.1021/ma0009350 CCC: $19.00
Published on Web 10/21/2000

the hydrodynamic approximation of ellipsoidal chain segments as equivalent spheres. In section 4, we apply the theory developed thus far to a practical problem, the trapping of DNA during gel electrophoresis, using data reported by Gurrieri et al.[4]

During gel electrophoresis DNA stretches and relaxes alternatively as it progresses through the gel. It is unknown how these conformation changes influence the mobility of DNA. For example, the treatment of Song and Maestre[3] of DNA sliding around a gel contact ignores the relaxation dynamics. Relaxation of stretched, tethered DNA is an excellent way of studying the hydrodynamic interactions between DNA and a gel, essentially independent of the charge of DNA and its ionic environment. Sections 5 and 6 deal with the relaxation of tethered, stretched DNA in gels, after the external electric field is turned off.

2. Solid Sphere Moving through Gel

Consider a solid sphere moving through a homogeneous liquid, as in sedimentation. The velocity u of the liquid around the sphere must satisfy the Navier−Stokes equations

$$\text{curl curl } u + \frac{1}{\eta}\nabla p = 0 \tag{1}$$

$$\text{div } u = 0 \tag{2}$$

where η is the viscosity of the liquid and p is the pressure. Equation 1 gives the local balance of forces on the liquid, that is, the viscous forces and the variations in pressure. Equation 2 expresses that the liquid is incompressible.

Now suppose that the sphere moves through an agarose gel. Then the gel fibers are in the flow field u and, hence, exert friction forces on the liquid which, in turn, modify the flow field. It would be difficult to treat the gel at any level that is physically realistic. Fortunately, we are mostly interested in the hydrodynamics of DNA when it is distributed over many of the pores, cells, and other inhomogeneities of the gel. So it is a fairly good approximation to treat the gel as a uniformly porous medium. Here we represent the gel by a collection of stationary beads in the liquid, each with friction factor f_b, and with concentration ν. When liquid flows though this porous medium with velocity u, friction with the beads produces a volume force on the liquid given by $-\nu f_b u$. A corresponding term appears in the local force balance which is now, instead of eq 1

$$\text{curl curl } u + \frac{\nu f_b}{\eta} u + \frac{1}{\eta}\nabla p = 0 \tag{3}$$

The incompressibility of the liquid, eq 2, is unchanged.

Following Debye[9] we set

$$\frac{\nu f_b}{\eta} = \frac{1}{L^2} \tag{4}$$

and we call L the shielding length of the gel. We expect that L is of the order of the average separation between fibers in the gel, and decreases with increasing agarose concentration. In gel electrophoresis, the shielding length L should be sufficient to characterize the gel. Appendix A gives the mathematics of solving eqs 2 and 3 for the problem at hand. In the next sections we need the friction coefficient f^* of the sphere with radius a in the gel

$$f^* = 6\pi\eta a\left(1 + \frac{a}{L} + \frac{a^2}{9L^2}\right) \tag{5}$$

We shall denote friction coefficients in a gel, such as in eq 5, with an asterisk. We need also the liquid velocity component u_z around the sphere when it moves with velocity v_0 along the z axis. In spherical coordinates r and θ, the angle between r and z, we have

$$u_z = v_0\left[-\frac{a^3}{2r^3} - \frac{3a^2L}{2r^3} - \frac{3aL^2}{2r^3} + \left(\frac{3a}{2r} + \frac{3aL}{2r^2} + \frac{3aL^2}{2r^3}\right)e^{-(r-a)/L}\right] + v_0\cos^2\theta\left[\frac{3a^3}{2r^3} + \frac{9a^2L}{2r^3} + \frac{9aL^2}{2r^3} - \left(\frac{3a}{2r} + \frac{9aL}{2r^2} + \frac{9aL^2}{2r^3}\right)e^{-(r-a)/L}\right] \tag{6}$$

Expansion of u_z for low porosity, that is, for large L, yields

$$u_z = v_0\left[\frac{3a}{4r} + \frac{a^3}{4r^3} + \frac{a}{L}\left(-1 + \frac{3a}{4r} + \frac{a^3}{4r^3}\right) + \frac{ar}{L^2}\left(\frac{9}{16} + \frac{a}{8r} + \frac{a^2}{16r^2}\right)\left(1 - \frac{a}{r}\right)^2\right] + v_0\cos^2\theta\left[\frac{3a}{4r} - \frac{3a^3}{4r^3} + \frac{3a^2}{4Lr}\left(1 - \frac{a^2}{r^2}\right) - \frac{ar}{L^2}\left(\frac{3}{16} + \frac{3a}{8r} + \frac{3a^2}{16r^2}\right)\left(1 - \frac{a}{r}\right)^2\right] + O\left(\frac{1}{L^3}\right) \tag{7}$$

The leading terms in eq 7 for $L = \infty$, in pure solvent, are the same as obtained from the Oseen tensor, $u_z = v_0(3a/4r)(1 + \cos^2\theta)$.

By modeling an agarose gel as a uniformly porous medium, the gel can be characterized by a single parameter, its hydrodynamic shielding length L. In the next section we discuss the dependence of the electrophoretic stretch of DNA on L.

3. Electrophoretic Stretch of DNA in a Gel

The present treatment parallels the one given in ref 7 of electrophoretic stretch of DNA in free solution. The differences are in the hydrodynamic details. We give here a fairly complete account because several aspects reappear in the relaxation treatment. We consider a DNA chain of persistence length P, modeled as a sequence of N freely rotating Kuhn segments, each of length $2P$. The chain is tethered at segment 1 to a fixed point in the gel, and is stretched in the positive z direction by an applied uniform electric field E. The tension in the stationary chain increases from the free segment $i = N$ to the tethered segment $i = 1$. As a result the segments closer to the tether point are oriented more parallel to the z axis. The orientation of segment i is given by the angle θ_i between segment i and the z axis. We evaluate the average value of θ_i from the tension T_i in segment i with the theory of Marko and Siggia[10] for the wormlike chain under constant tension. In terms of the dimensionless reduced tension

$$t_i = \frac{T_i P}{k_B T} \tag{8}$$

where k_BT is Boltzmann's constant times absolute temperature, Zimm's expression[11] for the average ori-

entation of segment i is

$$\cos\theta_i = \frac{0.6667t_i + 0.8080t_i^2 + 0.10365t_i^3}{1 + 1.1118t_i + 1.1076t_i^2 + 0.10365t_i^3} \qquad t_i \le 9 \quad (9a)$$

$$\cos\theta_i = 1 - \frac{0.49818}{t_i^{1/2}} \qquad t_i > 9 \quad (9b)$$

To prevent instabilities in the relaxation computations below, the original factor 0.5 in eq 9b has been replaced by 0.49818. This change makes the transition between eqs 9a and 9b at $t_i = 9$ smoother.

Equation 9 gives the extension of segment i in the z direction, $2P\cos\theta_i$, as a function of T_i. The tension T_i in segment i is the total force on the chain between segments $i + 1$ and the free end of the chain at $i = N$

$$T_i = \sum_{k=i+1}^{N} F_k \quad (10)$$

In eq 10 the force F_k on segment k is related to the electrophoretic velocity v_{el} of the segment, that is, the velocity of the single segment k if it were free to move in the field E. To derive F_k we introduce a sedimentation field such that it gives the single segment the compensating velocity $-v_{el}$. Therefore, when f_k^* is the friction coefficient of the single segment in a sedimentation experiment in the gel, the required sedimentation force is $F_{sed} = -f_k^* v_{el}$. Since the segment is stationary, the total force on it must vanish, giving $F_k + F_{sed} = 0$. So we find

$$F_k = -F_{sed} = f_k^* v_{el} \quad (11)$$

In eq 11 the electrophoretic velocity v_{el} and the friction coefficient f_k^* both depend on the orientation of segment k in the applied field. Let $v_{||}$ be the electrophoretic velocity parallel to the long segment axis and $v_\perp$ that perpendicular to it, given by eqs 24 and 25 of ref 7. We assume that the influence of the gel on the electrophoretic mobility of a single segment is insignificant, as justified below with Figure 1. Then, adding the force components on segment k in the z direction, one obtains[7]

$$F_k = v_{||} f_{||}^* \cos\theta_k + v_\perp f_\perp^* \sin\theta_k = \frac{\epsilon_0 D\zeta E}{\eta}\left(f_{||}^* \cos^2\theta_k + \frac{2}{3} g_\perp f_\perp^* \sin^2\theta_k\right) \quad (12)$$

where ϵ_0 is the permittivity of vacuum, D the dielectric constant of the solvent, ζ the surface potential of the DNA cylinder, $f_{||}^*$ the friction coefficient of a segment for motion in the gel parallel to the long axis, and $f_\perp^*$ for motion in the gel perpendicular to the long axis of the segment, and $g_\perp$ is a numerical factor of order unity. Equation 12 gives the force F_k on a single, isolated segment in the gel, held stationary in the external field E. Is F_k different for segments in a chain? That depends on the intersegment interactions through the surrounding gel which are very different in sedimentation and electrophoresis. We first discuss these interactions in free solution.

The intersegment interactions depend on the flow field around a single segment. An example of a flow field around a charged sphere in electrophoresis is presented in Figure 1, computed for a sodium dodecyl sulfate micelle in 0.03 M NaCl as based on the electrophoresis theory of Wiersema.[12] The length and the direction of the arrows give the liquid velocity at their starting point in a square grid. The solid sphere moves with the velocity of the arrows at its surface. Here the total flow has two components. First, the Stokes field resulting from the electric force on the charge fixed to the sphere and, second, the backflow due to the electric force on the neutralizing ionic atmosphere around the sphere. The pattern in Figure 1 reveals that the sum of these two velocities decreases fast with the radial distance r from the center of the sphere, on average approximately as $e^{-\kappa r}/r$, where $1/\kappa$ is the Debye length of the ionic solution. The velocity decay around a DNA segment in electrophoresis is similarly rapid. Since the segment length of 1000 Å is many times the Debye length, it is a good approximation to neglect the intersegmental interaction in electrophoresis. This is not so in sedimentation.

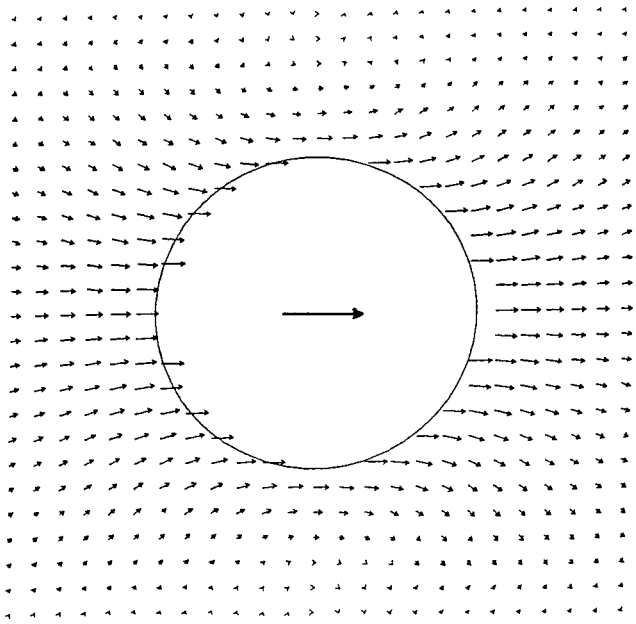

Figure 1. Hydrodynamic flow around micelle of sodium dodecyl sulfate in 0.03 M NaCl solution during electrophoresis.[13]

Figure 2 shows the flow field in free solution around a sphere in sedimentation, calculated from Stokes' equations,[14] that is from eqs A18 and A19 in Appendix A for $L = \infty$. The liquid velocity decreases slowly with the distance from the sphere, on average as $1/r$. A similar slow decay occurs around the ellipsoidal segment in sedimentation. So in the stretched chain the flow fields, generated by the sedimentation forces on the other segments, reach segment k to some extent and thus modify the net force on it. The result is that the force F_k is less than predicted by eq 12. We now consider the hydrodynamic details.

For hydrodynamic purposes a segment of the DNA chain is treated as a prolate ellipsoid with long axis $2P$, the contour length of the segment, and short axis $c = d\sqrt{1.5}$ where d is the diameter of the hydrodynamic DNA cylinder. This choice of c leaves the volume of the segment unchanged. Oberbeck[15] has treated the hydrodynamic resistance and viscous flow in free solution around a solid ellipsoid with three different axes. We have specialized the results to those for the prolate

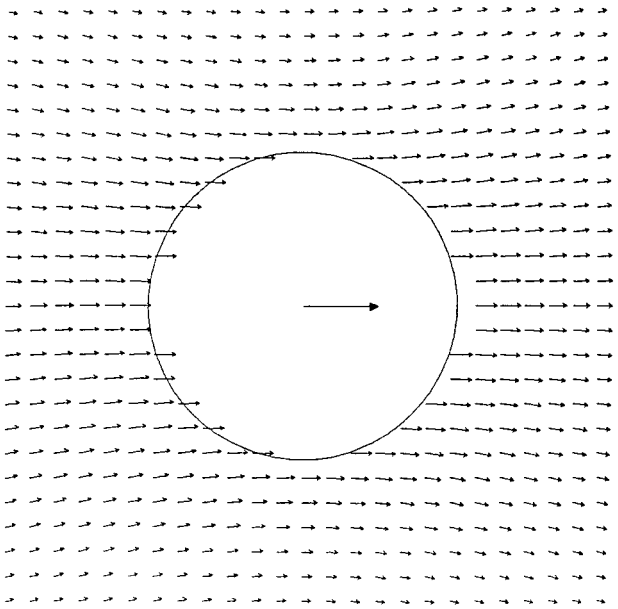

Figure 2. Stokes hydrodynamic flow around moving sphere.[13]

ellipsoid. The results, in terms of the axial ratio $\phi = 2P/c$, are consistent with expressions in the literature[16]

$$f_{\parallel} = \frac{4\pi\eta c}{\left[-\frac{\phi}{\phi^2-1} + \frac{2\phi^2-1}{(\phi^2-1)^{3/2}}\ln(\phi+\sqrt{\phi^2-1})\right]} \quad (13)$$

$$f_{\perp} = \frac{8\pi\eta c}{\left[\frac{\phi}{\phi^2-1} + \frac{2\phi^2-3}{(\phi^2-1)^{3/2}}\ln(\phi+\sqrt{\phi^2-1})\right]} \quad (14)$$

As shown later, eqs 13 and 14 are used in eq 12 for the force F_k on segment k. They are also used in the friction coefficient f_k of segment k with orientation angle θ_k, required for the interaction between segments. In free solution the relation for segment k is, see eq 5 of ref 7

$$f_k = f_{\parallel}\cos^2\theta_k + f_{\perp}\sin^2\theta_k \quad (15)$$

The expressions for the liquid velocity around the ellipsoid are rather unwieldy and are not reproduced here. Although the results have been coded for computation, their use in the interaction treatment would require too much computer time. Therefore, the interaction calculations are carried out for equivalent spheres, that is, the ellipsoids in eqs 13 and 14 are treated as solid spheres with radii $a_{\parallel}$ and $a_{\perp}$ defined with

$$6\pi\eta a_{\parallel} = f_{\parallel} \qquad 6\pi\eta a_{\perp} = f_{\perp} \quad (16)$$

and segment k is modeled as a sphere with radius a_k

$$a_k = a_{\parallel}\cos^2\theta_k + a_{\perp}\sin^2\theta_k \quad (17)$$

This substitution does not change the friction of the segment in eq 15, only the liquid flow around it. The approximation is tested by comparing the liquid velocity along the z axis caused by the moving ellipsoid with the slightly lower liquid velocity generated by the equivalent sphere, that is, with u_z from eq 7 for $\cos\theta = 1$ and $L = \infty$. The segments are modeled as a prolate ellipsoid with long axis $2P = 1000$ Å and short axis $c = 22\sqrt{1.5}$ Å, as

Table 1. Liquid Velocity Ratio around Sphere and Ellipsoid on the *z* Axis

n	$\theta = 0$	$\theta = \pi/2$
1	0.9081	0.9161
2	0.9782	0.9804
3	0.9904	0.9914
4	0.9946	0.9951
5	0.9965	0.9969
6	0.9976	0.9979
7	0.9982	0.9984
8	0.9987	0.9988
9	0.9989	0.9990
10	0.9991	0.9992

appropriate for B-DNA. For orientation parallel to the z-axis eqs 13 and 16 give a radius $a_{\parallel} = 87.50$ Å for the equivalent sphere, for perpendicular orientation eqs 14 and 16 give a radius $a_{\perp} = 138.68$ Å. With the center of ellipsoid and spheres at $z = 0$, Table 1 gives the velocity ratio at distances z that are multiples of the ellipsoid axes, that is, at $z = n \times 2P$ for parallel orientation, $\theta = 0$, and at $z = nc$ for perpendicular orientation, $\theta = \pi/2$. Table 1 shows that the sphere approximation gives interactions that for nearest neighbor segments, $n = 1$, are about 10% too small, for next nearest neighbor segments, $n = 2$, about 2% too small. For larger distances along the chain the errors become insignificant. We conclude that the equivalent sphere representation of the segments is a good approximation.

So far the hydrodynamic development has been for segments in free solution. With the introduction of equivalent spheres we can now change to hydrodynamics in a gel by using eq 5 for the friction of the equivalent spheres and eq 6 for the liquid flow around them. Equations 5 and 15−17 yield for the friction coefficient of a single chain segment in the gel

$$f_k^* = 6\pi\eta a_{\parallel}\left(1 + \frac{a_{\parallel}}{L} + \frac{a_{\parallel}^2}{9L^2}\right)\cos^2\theta_k + 6\pi\eta a_{\perp}\left(1 + \frac{a_{\perp}}{L} + \frac{a_{\perp}^2}{9L^2}\right)\sin^2\theta_k \quad (18)$$

The intersegment interaction requires the conformation of the chain. As explained in ref 7, this conformation is obtained with the values $\cos\theta_i$ from eq 9, and assuming random orientation of the segments around the z axis. This gives the distance $r = r_{kj}$ between segments k and j and the angle $\theta = \theta_{kj}$ between r_{kj} and the z axis required in eq 6. We rewrite eq 6 as

$$u_z = v_0[h_1(r, a, L) + \cos^2\theta\, h_2(r, a, L)] \quad (19)$$

Applied to the flow generated by the sedimentation force $-F_j$ on segment j, we have with eq 11 in eq 19

$$v_0 = \frac{-F_j}{f_j^*} \quad (20)$$

and for the relevant velocity $u_z = \Delta u_{kj}$ at segment k

$$\Delta u_{kj} = \frac{-F_j}{f_j^*}[h_1(r_{kj}, a_j, L) + \cos^2\theta_{kj}h_2(r_{kj}, a_j, L)] \quad (21)$$

The total liquid velocity in the z direction at segment k is

$$u_k = \sum_{j=1}^{N} \Delta u_{kj} \quad j \neq k \tag{22}$$

The extra force $f_k^* u_k$ is the interaction correction in eq 12 which becomes

$$F_k = \frac{\epsilon_0 D \zeta E}{\eta}\left(f_{\|}^* \cos^2\theta_k + \frac{2}{3} g_\perp f_\perp^* \sin^2\theta_k\right) - f_k^* \sum_{j=1}^{N} \frac{F_j}{f_j^*}[h_1(r_{kj}, a_j, L) + \cos^2\theta_{kj} h_2(r_{kj}, a_j, L)] \quad j \neq k \tag{23}$$

For $L = \infty$, eq 23 is consistent with eq 29 of ref 7. The conformational angles θ_i of the segments and the tensions T_i can now be obtained from eqs 9, 10, and 23 with an iterative computation.

We can now estimate the shielding length L of agarose gels from experiments by Gurrieri et al.[4] These stretching experiments of 97 kbp B-DNA were carried out in a buffer of 45 mM Tris borate/1mM EDTA, at pH = 8.3, with electric fields up to 20 V/cm. From capillary electrophoresis experiments of B-DNA in the same buffer by Stellwagen et al.,[17] and the long rod electrophoresis theory,[18,19] we compute a surface potential $e\zeta/kT = 4.07$ and an electrophoretic factor $g_\perp = 0.495$. With the persistence length of B-DNA, $P = 500$ Å, the tether force T_1 was computed in gels with shielding length $L = 10^{-8}$–10^{-4} m. The results are plotted in Figure 3 for electric fields $E = 10$ and 20 V/cm. The tether force T_1 in free solution, for $L = \infty$, differs not significantly from that for $L = 0.01$ m, where we find $T_1 = 0.920$ pN for $E = 10$ V/cm and $T_1 = 2.246$ pN for $E = 20$ V/cm. With these values the experimental ratio[4] T_1(gel)/T_1(free solution) = 4, indicated by the horizontal dashes in Figure 3, gives about $L = 5 \times 10^{-8}$ m for $E = 10$ V/cm and $L = 3 \times 10^{-8}$ m for $E = 20$ V/cm. The present experimental information allows only a preliminary estimate of the hydrodynamic shielding length in a 1.2% agarose gel, about $L = 4 \times 10^{-8}$ m. We shall use this result for L in the rest of the paper.

4. Application of Electrophoretic Stretch Theory to the Trapping of DNA in Gel Electrophoresis

With the theory discussed so far we calculate the critical trapping force T_{crit} of DNA. The experimental data in Figure 1 of Gurrieri et al.[4] indicate that the relation between DNA size and the critical field strength, E_{crit}, for trapping in a 1% agarose gel is given by

$$\text{DNA size} \times E_{crit} = 7000 \text{ kbp V/cm} \tag{24}$$

where E_{crit} is the field strength sufficient to cause 50% trapping of a band over a 1 cm path. We assume that trapping is the immobilization of DNA in a U-shape as pictured in Figure 4, with legs of contour length l_1 and l_2 in the field direction, except where the DNA bends around the gel contact. The point of contact serves as a tether point to treat the tensions in the left and right legs of the DNA. At the vertex, the tether forces are directed in opposite directions along the DNA, perpendicular to the electric field. The tether forces are approximately proportional to the length of the legs, varying with the location along the DNA where it is

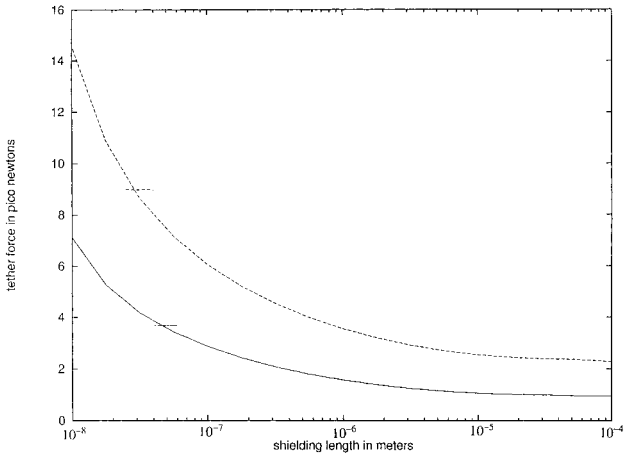

Figure 3. Tether force T_1 as a function of hydrodynamic shielding length L for 97 kbp DNA in 1/2 TBE buffer in electric field $E = 10$ (lower curve) and 20 V/cm (upper curve). Horizontal dashes for experimental ratio[4] T_1 (gel)/T_1 (free solution) = 4.

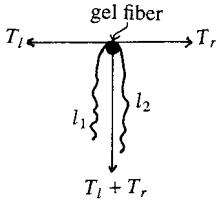

Figure 4. U-shaped DNA hooked over gel fiber, with tether forces T_l and T_r, loading force $T_l + T_r$ at contact, and lengths l_1 and l_2 of inverted U.

Table 2. Critical Trapping Force $T_l + T_r$ in Piconewtons (pN) as a Function of DNA Size

DNA size, kbp	E_{crit}, V/cm	$T_l + T_r$, pN
500	14	29.64
250	28	29.67
125	56	29.51
62.5	112	29.34
31.25	224	28.69

Table 3. Critical Trapping Force for 125 kbp DNA with $E_{crit} = 56$ V/cm as a Function of Asymmetry of Chain Configuration

$l_1/(l_1 + l_2)$	$T_l + T_r$, pN
0.1	29.63
0.2	29.41
0.3	29.28
0.4	29.25
0.5	29.22

trapped. The sum of the tether forces is equal to the loading force normal to the DNA/gel fiber interface. As shown below in Table 3, this sum is nearly independent of the location of the gel contact along the DNA chain. At the critical field strength we identify the sum of the tether forces with the critical trapping force

$$T_{crit} = T_l + T_r \tag{25}$$

A possible mechanism of trapping is as follows. For a small loading force, at low field, DNA and the gel fiber remain fully hydrated, with essentially liquid or lubricated friction at the contact.[6,20] When the loading force increases, water is gradually squeezed out of the contact area, and eventually we have solid friction between DNA and the gel fiber.[5,20] At the transition from lubricated to solid contact the friction coefficient in-

creases sharply,[20] leading to immobilization of the DNA. This hydration/friction mechanism is reversible. When the external field is lowered below E_{crit}, the trapped DNA will rehydrate, become mobile again, and slip off the gel contact. However, trapping might not be a single event. DNA might unwind at the gel contact, before or after trapping, perhaps aided by the curvature of the DNA, making reversibility less likely. One expects that the onset of such unwinding depends on the salt concentration, just as the overstretching of dsDNA.[21] If unwinding DNA is part of the trapping process, adding salt should increase the critical trapping force T_{crit}.

In the following calculations, we assume the same ionic conditions as in Figure 3. We use eqs 9, 10, and 23 to compute the tether forces T_l and T_r for the stationary legs at the gel contact, for DNA sizes from 500 kbp down to 31.25 kbp, with E_{crit} increasing from 14 to 224 V/cm in accordance with eq 24. Table 2 shows the critical trapping force $T_{crit} = T_l + T_r$ for the symmetrical U-shape, $l_1 = l_2$. Table 3 presents T_{crit} for DNA of 125 kbp trapped at various points along the chain in a field of $E_{crit} = 56$ V/cm. The results show that T_{crit} does not vary significantly with DNA size or with the asymmetry of the U-shape. This shows that the proposed trapping mechanism is consistent with the experimental relation eq 24. The present result for the trapping force, about $T_{crit} = 29$ pN, is substantially higher than the value of 15 pN by Gurrieri et al.[4] The reason is that in eq 1 of their paper the value 15 pN is the tether force in one leg only for the symmetrical U-shape, while the critical loading force at the gel-DNA contact is the sum of the tether forces of both legs of the U. So the value $T_l + T_r = 2 \times 15 = 30$ pN should be compared to our value of 29 pN. Given the different calculations, the two values are remarkably close.

The mechanism of trapping discussed above allows trapping at any point along the DNA fiber. On the other hand, the interpretation of Gurrieri et al.[4] suggests trapping near the center of the DNA. These authors elaborate on nicks in the DNA as favorite sites for trapping DNA around a gel fiber. If nicks are important, one does not expect a significant dependence of the critical trapping force on the salt concentration. Furthermore, if structural changes such as unwinding or nicks are the main cause of trapping, one expects E_{crit} to relate to the tension in the chain, T_r or T_l as implied by Gurrieri et al.[4] But if trapping is caused by increased friction with the gel, E_{crit} should be related to the normal force $T_r + T_l$ at the gel contact as in eq 25. In summary, there are two experiments to shed further light on the mechanism of trapping, the effect of salt on E_{crit}, and the sensitivity of E_{crit} to the location along the trapped chain.

One of the features in DNA gel electrophoresis is the relaxation of DNA. In addition, single molecule relaxation experiments give information on the hydrodynamic shielding length L of the gel. The next section deals with the relevant theory.

5. Relaxation of Tethered DNA after Stretching

Section 3 gives a theory for the electrophoretic stretch of DNA tethered in a gel and subjected to a uniform electric field. We now consider what happens when the electric field is turned off. In particular we consider the time dependence of the end-to-end distance and of the tether force along the z axis, the direction of stretch. A stretched chain has fewer configuration than a less extended chain. Therefore, when the field is turned off, the chain is contracted by an entropic force which is related to its extension. The rate at which this happens depends on the tension in the chain. Our main tool here is the theory of Marko and Siggia[10] which gives in eq 9 a relation between the tension in a chain, or in a chain segment, and its relative extension. Although derived for static conditions, we assume that, when a stretched chain relaxes, kinetic effects may be neglected and eq 9 is still valid. In other words, eq 9 gives the instantaneous relation between relative extension and tension which are now time-dependent quantities. Below we need the tension T_i in segment i as a function of its relative extension $\cos\theta_i$, the inverse of eq 9. For given $\cos\theta_i$ it is simple to interpolate T_i in a list of paired $(\cos\theta_i, T_i)$ values computed from eq 9.

At any time, the force on the tether point is determined by the tension in the tethered end of the chain which is related to the relative chain extension at the tethered end. So the change of this local chain extension with time gives the relaxation of the tether force. The relaxation of the end-to-end distance, on the other hand, depends on what happens to the tension along the entire chain. So we have two different relaxation processes which both depend on the DNA/gel hydrodynamics. Both relaxation rates change continuously with time. To simplify the treatment we shall keep the rates constant over short time intervals Δt. These intervals must be short enough to prevent instabilities in the relaxation process. We first discuss the behavior of the chain during a time interval Δt.

Similar to liquid flow through a tube caused by a pressure *gradient*, the relaxation contraction of DNA is caused by the *gradient* of the tension in the chain. We have divided the DNA chain into segments $i = 1$ to N in which the tension T_i is constant. The local tension gradient at segment i is supposed to be proportional to $T_i - T_{i+1}$. This means that the driving force for shortening segment i is the tension difference $\Delta T_i = T_i - T_{i+1}$. When this entropic force contracts segment i at the rate v_i, the free end of the chain, segments i to N, is dragged through the gel with the same velocity v_i, and with a total friction force equal to ΔT_i. For known friction this force balance yields v_i. The friction force we need here is the sum of the friction forces F_k exerted on segments $k = i$ to N when this free end of the chain moves through the gel with constant velocity v_i and with constant configuration. Without hydrodynamic interaction between the segments we have

$$F_k = f_k^* v_i \tag{26}$$

with f_k^* given by eq 18. The second term of eq 23 gives the hydrodynamic interaction between the segments in the entire chain, resulting from the drag forces $-F_j$ on chain segment j. At present we need only the intersegment interaction in the free end of the chain, with index j running from i to N. So with eq 26, and changing the summation of the intersegment term of eq 23, we have

$$\Delta T_i = T_i - T_{i+1} = \sum_{k=i}^{N} F_k = \sum_{k=i}^{N}\left\{ f_k^* v_i - f_k^* \sum_{j=i}^{N} \frac{F_j}{f_j^*}[h_1(r_{kj}, a_j, L) + \cos^2\theta_{kj} h_2(r_{kj}, a_j, L)]\right\} \qquad j \neq k \tag{27}$$

The set of eqs 27, one for each i, is solved for the v_i values by an iterative computation for constant chain conformation, subject to the condition that neighboring spheres cannot overlap, $r_{kj} \geq a_k + a_j$.

The relaxation computation starts with the set of cos θ_i and T_i values of the electrophoretically stretched DNA. After the electric field is turned off at time $t = 0$, the relaxation velocity v_i of each segment $i = 1$ to N decreases continuously with time t until the segment is relaxed completely, when cos $\theta_i = 0$, $T_i = 0$, and $v_i = 0$. As already mentioned above, we approximate the smooth $v_i - t$ curves by step functions with many small time steps Δt. During each time step all velocities v_i are kept constant. The chain configuration is updated after each time step as follows. During an interval Δt the extensions of all relaxing segments i are decreased by $v_i \Delta t$, giving a new set of cos θ_i values. These are used with the inverse of eq 9 to find new tensions T_i. The iterative solutions of eq 27, one for each segment i, now yield a new set of relaxation velocities v_i, the input for the next time step Δt. This cyclic computation is terminated for any segment i when its relaxation is complete. The termination time increases from $i = N$ to $i = 1$. Adding the time steps and, at any step Δt, the segment extensions gives the relaxation curve of chain extension vs time. The same computation gives also the change of the tether force, T_1 for segment $i = 1$, with time.

With eqs 26 and 27 the chain relaxes toward a random, flat conformation in the xy plane at $z = 0$. This is unrealistic because we have neglected Brownian motion of the relaxing chain in the z direction. In a treatment of hydrodynamic stretch Zimm[11] has introduced effects of diffusion into weakly stretched chains, the small force part of eq 9, with the three-dimensional, unstretched coil as the limit. In our approach, it is difficult to introduce segment diffusion along the z axis during relaxation because it may create persistent tension gradients of the wrong sign, $T_{i+1} > T_i$, and thus might cause computational instabilities. Therefore, we account for diffusion only for the segments that have relaxed completely, from segments i_0 to N. For these segments the spatial direction is chosen randomly. Thus, the relaxed end of the chain, from segments i_0 to N, forms a random coil around the end of the unrelaxed chain at $z = z(i_0)$. Treating this random coil as a uniformly filled sphere, statistics of the freely jointed chain give $R = (P/3)\sqrt{10(N-i_0)}$ for the average radius of the sphere. We add the distance R to the extension $z(i_0)$ of the relaxing chain.

The most time-consuming part of the computation is recalculating the friction coefficients. Fortunately, their change with chain extension is small so that updating them only once in every 10 time steps does not cause significant error.

6. Relaxation Calculations and Results

The success of the cyclic computation depends on the choice of the time steps Δt. The computation becomes unstable for too large values of Δt, due to the appearance of tension gradients of the wrong sign, $T_i < T_{i+1}$. Such instabilities can be avoided by choosing Δt sufficiently small, proportional to the friction coefficient of the part of the chain for which the relaxation has been completed, and for highly stretched chains inversely proportional to the tether force T_1. This makes the time steps longer when the relaxation process proceeds.

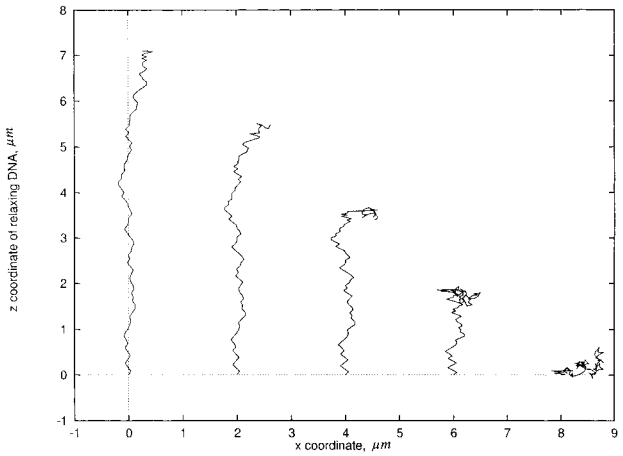

Figure 5. Calculated conformations of dsDNA during relaxation.

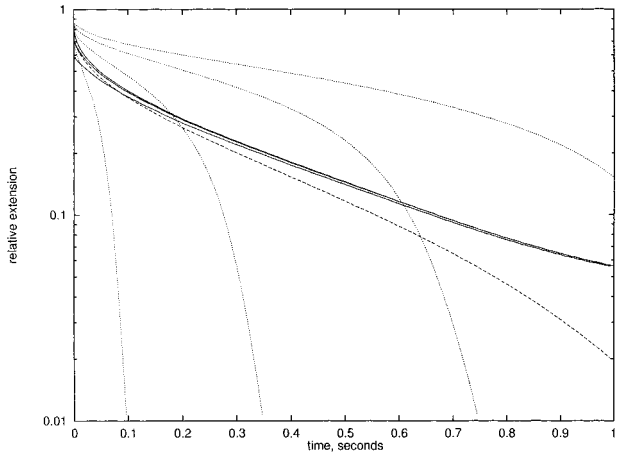

Figure 6. Relative extension−time curves of DNA with $N = 100$ segments relaxing in gel with shielding length $L = 4 \times 10^{-8}$ m in buffer solution as in Figure 3. Solid curves from top to bottom: Initial stretching in electric field of 20, 10, and 5 V/cm. Dotted curves: Single segment relaxation, from left to right for segment $i = 75$, 50, 25, and 1. Dashed curve: Relaxation theory without diffusion.

Shortening the time steps of a stable computation does not change the results significantly. The computations in this paper are for a total of about 250−4200 time steps per relaxation curve, depending on the number of segments per chain, $N = 50-326$.

Figures 5−8 are for dsDNA with $N = 100$ segments, each of length $2P = 10^{-7}$ m in a gel with shielding length $L = 4 \times 10^{-8}$ m. The tethered DNA is first stretched in an electric field under the ionic conditions of Figure 3. Figure 5 depicts some of the successive conformations of a relaxing DNA molecule, tethered at $z = 0$. The conformation of the lower part of the chain changes slowly because the random sequence for the x and y coordinates is unchanged during relaxation of the segments. On the other hand, the conformation of the fully relaxed blob at the free chain end is randomized anew before each update of the friction factors. The appearance of a blob or compact ball at the end of a relaxing chain agrees with microscopic observations on stained DNA by Perkins et al.[22]

The solid curves in Figure 6 are extension−time curves after stretching in a field of 5, 10, or 20 V/cm. The initial fast relaxation of the more highly stretched DNA agrees with experimental observations.[22] In the later stages of relaxation the curves are close together,

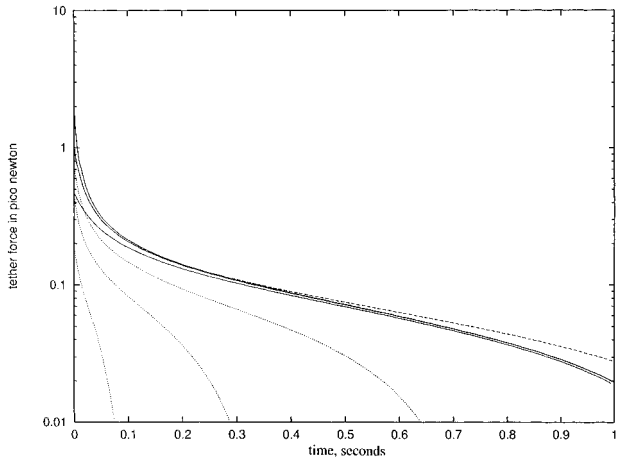

Figure 7. Relaxation of tension T_i vs time in DNA under conditions of Figure 6. From left to right in segments $i = 75$, 50, 25, and 1 (=solid curve for tether force).

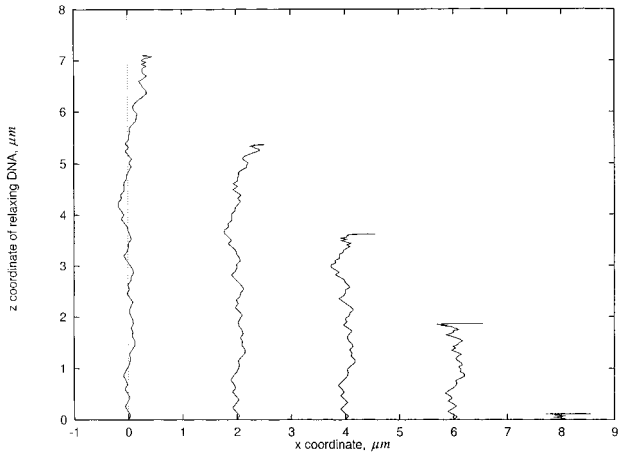

Figure 8. Calculated conformations of dsDNA during relaxation without diffusion.

showing that the effect of the extent of initial stretching is rather small. The dotted curves in Figure 6 give the relaxation of single segments, from left to right for $i =$ 75, 50, 25, and 1 segments from the tethered end. For smaller i the segment relaxes slower because the free end of the chain, segments i to 100, is longer and, hence, has a larger friction coefficient. The relaxation rate of the total chain is the average of the rates of the single segments. Figure 7 shows the relaxation of the tension for the same conditions as in Figure 6. The dotted curves give the tension, from left to right in segments $i = 75$, 50, and 25. The solid curves give the tension in the first segment, the tether force for initial stretching with 5, 10, and 20 V/cm. As in Figure 6, the influence of the initial stretching shows up mostly in the early part of the relaxation curve.

The dashed curves in Figures 6 and 7 are for the same conditions as the middle solid curve, but with omission of the diffusion terms in the relaxation process. Figure 8 shows some of the corresponding conformations. Instead of the three-dimensional blob of Figure 5, we have now a flat configuration of the fully relaxed chain end, viewed as a line in the $z-x$ plane, at the end of the relaxing part of the chain at $z(i_0)$. Introducing diffusion has two effects on the calculated relaxation. First, as shown in Appendix B, the three-dimensional configuration of the relaxed chain end has on average a smaller friction coefficient than its flat, two-dimensional con-

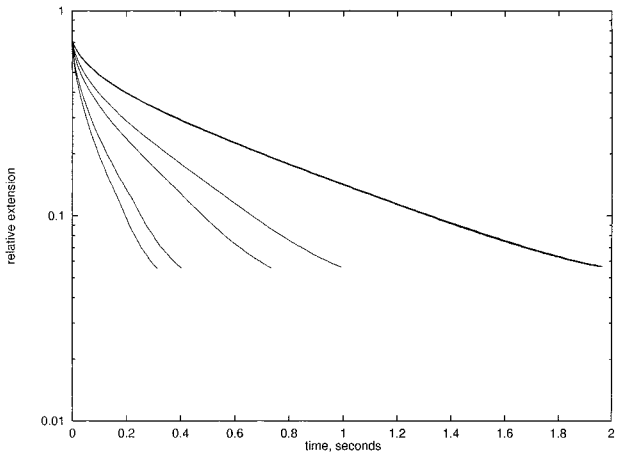

Figure 9. Relaxation curves of DNA, 100 segments, in different porous media in buffer of Figure 3. From left to right shielding length $L = 0.1$, 10^{-6}, 10^{-7}, 4×10^{-8}, and 10^{-8} m. Plots for five different random number sequences in heavy curve on right.

figuration. This increases the relaxation rate, as observed in Figure 7 for the tether force. The extension-time curve in Figure 6 is modified by a second diffusion effect. Here we add the radius of the three-dimensional blob to the extension $z(i_0)$, and thus slow the observed relaxation process, overcompensating the friction effect. The present approximation neglects the diffusion of the relaxing part of the chain and ignores excluded volume and charge effects in estimating the radius of the blob. The total effect of diffusion on relaxation is, however, not very large so that the present approximation is probably adequate.

Figure 9 shows that the porosity of the medium has a considerable influence on the relaxation time. All curves are for $N = 100$ segments, from left to right in porous media with shielding length $L = 0.1$, 10^{-6}, 10^{-7}, 4×10^{-8}, and 10^{-8} m. For $L = 0.1$ m, the medium behaves as pure solvent. The heavy curve for $L = 10^{-8}$ m consists of five plots based on five different random number sequences used in the computation. We see that the influence of the particular chain conformations on the relaxation results is insignificant.

The effect of chain length is demonstrated in Figure 10 for chains with $N = 50$, 100, and 200 segments in a gel, solid curves for $L = 4 \times 10^{-8}$ m, and in pure aqueous solvent, dashed curves for $L = 0.1$ m. To test scaling the abscissa is proportional to t/N^{α} with α chosen for optimum collapse of the three curves in each set. In Figure 10, we have used $\alpha = 1.85$ in the gel and $\alpha =$ 1.70 in pure solvent. The value in water agrees fairly well with values derived from experiments in pure solvent by Perkins et al.[22] It is obvious in Figure 10 that the length scaling of relaxation is far from perfect. For good scaling in early and middle ranges, the relaxation in the later time range is relatively slower for the shorter chains. The reason is the relatively larger contribution of diffusion for shorter chains. The radius of the relaxed blob is proportional to $(N - i_0)^{1/2}$ and, hence, adds more to the relative extension of shorter chains. Without this contribution of diffusion, scaling is much improved, as shown in Figure 11 for the relaxation of the tether force, with $\alpha = 1.97$ in the gel and $\alpha = 1.82$ in pure solvent. The diffusion has only a minor effect on the tether force, through the friction coefficient of the chain. We note that the scaling coefficients for length and force relaxation are different,

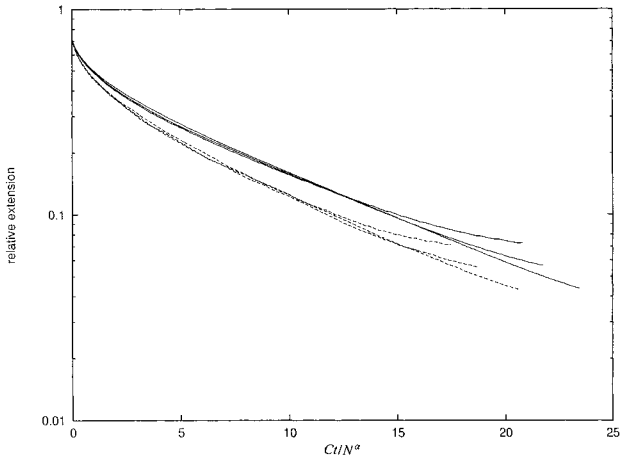

Figure 10. Extension relaxation for various sizes of dsDNA plotted vs Ct/N^{α}. Solid curves: In gel with $L = 4 \times 10^{-8}$ m, $C = 1.1 \times 10^{5}$, and $\alpha = 1.85$. Dashed curves: In aqueous solvent, $C = 1.5 \times 10^{5}$ and $\alpha = 1.70$. From top to bottom in each set $N = 50$, 100, and 200.

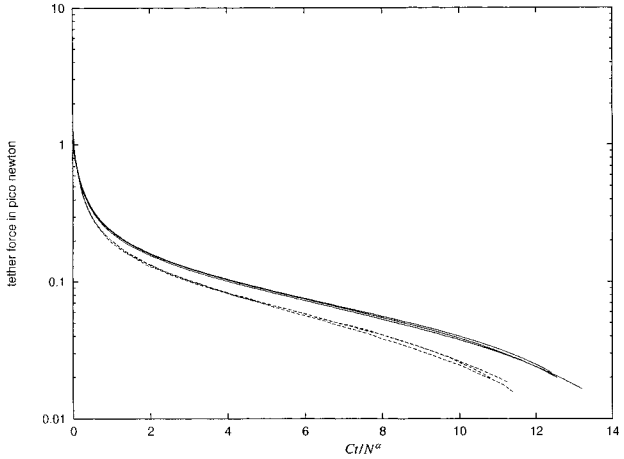

Figure 11. Relaxation of tether force of dsDNA with $N = 50$, 100, and 200 plotted vs Ct/N^{α}. Solid curves: In gel with $L = 4 \times 10^{-8}$ m, $C = 1.1 \times 10^{5}$ and $\alpha = 1.97$. Dashed curves: In aqueous solvent, $C = 1.5 \times 10^{5}$ and $\alpha = 1.82$.

showing that the two relaxation processes are not directly related.

In Figures 12−14 the theory is compared with the experimental data in Figure 2C of the paper by Perkins et al.[22] for DNA fibers stained with YOYO-1, in an aqueous buffer solution with a viscosity of 15 cP. Each fiber was attached to a 1-μm polystyrene bead held in a laser trap in the center of a 30−40 μm wide cell. With the bead stationary, the cell was first moved steadily at 20 μm/s to stretch the DNA chain hydrodynamically, until the cell motion was stopped at time $t = 0$. In Figures 12−14 the chain extension is given as a function of t for DNA of different lengths, with each point the average of four or five different length measurements. For each fiber the contour length was calculated from the initial extension, using the earlier theory[7] and assuming that the persistence length of stained DNA is 650 Å.[23] The contour lengths are 42.4, 23.5, and 9.2 μm for the fibers initially stretched to 39.1, 21.1, and 7.7 μm respectively in the 20 μm/s flow. The agreement between theory and experiment is fairly good, about the same in the three cases considering the difference in time axis. The main systematic difference between theory and experiment is a shift of the time axis of the order of a second.

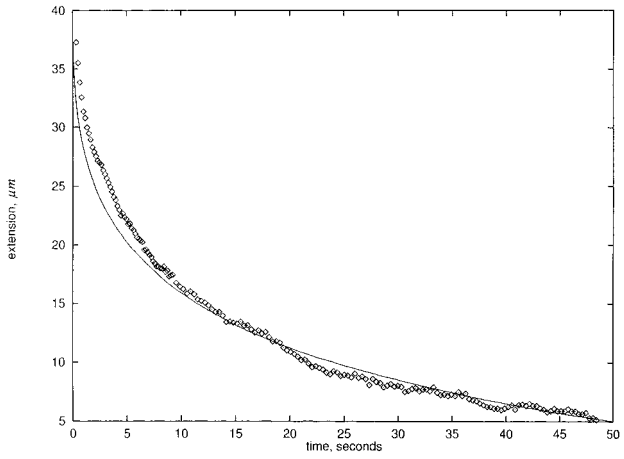

Figure 12. Relaxation of 42.4 μm long, stained DNA in liquid with viscosity of 15 cP, stretched to 39.1 μm in 20 μm/s flow. Solid line: Present theory. Points: From experiments by Perkins et al.[22]

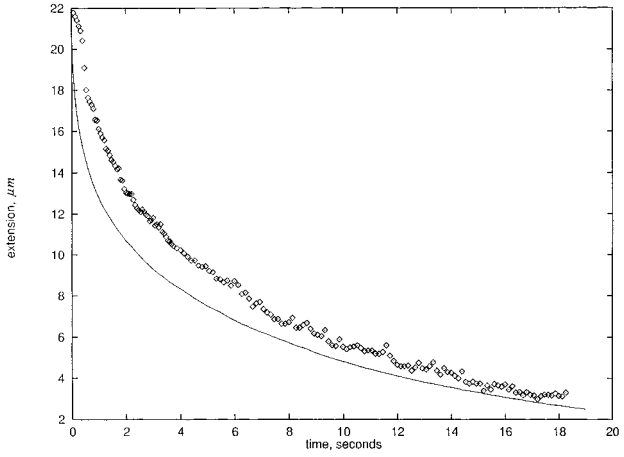

Figure 13. Relaxation of 23.5 μm long, stained DNA in liquid with viscosity of 15 cP, stretched to 21.1 μm in 20 μm/s flow. Solid line: Present theory. Points: From experiments by Perkins et al.[22]

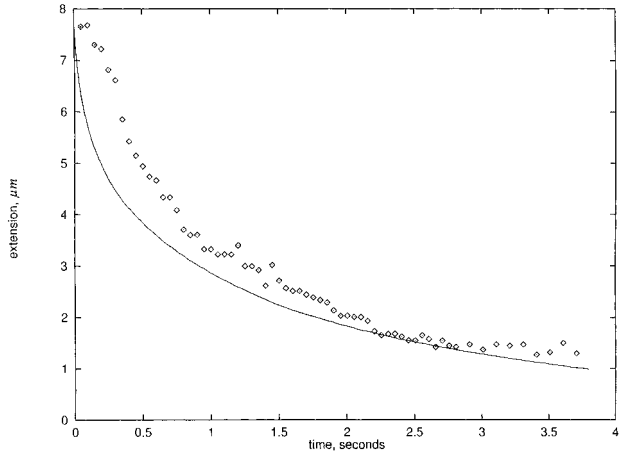

Figure 14. Relaxation of 9.2 μm long, stained DNA in liquid with viscosity of 15 cP, stretched to 7.7 μm in 20 μm/s flow. Solid line: Present theory. Points: From experiments by Perkins et al.[22]

Figure 15 shows relaxation curves of 10 μm long DNA, assuming various persistence lengths, from left to right $P = 500$, 650, and 800 Å. It appears that theoretical relaxation curves are sensitive to errors in the assumed persistence length. Nevertheless, it is obvious from

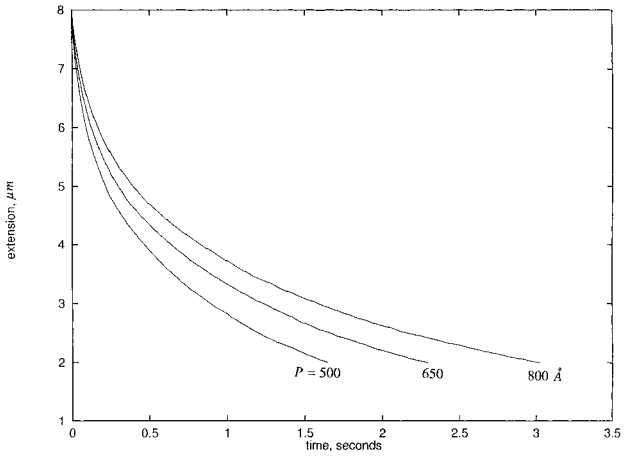

Figure 15. Relaxation−time curves of 10 μs long dsDNA in liquid with viscosity of 15 cP for various persistence lengths. From left to right $P = 500$, 650, and 800 Å.

Figure 15 that the discrepancy between theory and experiment in Figures 12−14 is not due to the uncertainty in the assumed persistence length, $P = 650$ Å. A possible explanation for an uncertainty of the experimental time is given in the next section.

7. Discussion

The theory of polymer dynamics is frequently based on a sequence of beads connected by springs, as treated in particular by Zimm.[24] Although very successful for hydrodynamic problems, this model is not very suitable for treating electrophoretic problems of polyelectrolytes. Because of short-range effects of electrical origin one prefers a model that resembles the polyelectrolyte chain more closely than a string of beads. A cylinder model allows a more accurate treatment of the steep gradients of the liquid velocity and small ion concentrations in the ionic atmosphere surrounding the charged chain. We have used the cylinder model also for the relaxation problem because of possible applications to relaxation of DNA during gel electrophoresis.

We have not compared the present work with the Rouse and Zimm theories because their linear models do not apply to the highly extended chains treated here, as discussed in detail by Perkins et al.[22]

In the experiments of Perkins et al.[22] shown in Figures 12−14, the 1 μm bead moved with the stretched DNA through the solution with a constant velocity of 20 μm/s. This motion of the bead produced around it a liquid flow similar to the Stokes flow shown in Figure 2. The difference, however, is that the closed cell of finite size forced a backflow of liquid at larger distance from the bead so as to make the total flow through any cross section of the cell vanish. When at $t = 0$ the cell was stopped with respect to the bead, the perturbation flow persisted momentarily, to fade away with a relaxation time determined by the geometry of the cell. After $t = 0$ the stationary bead interfered with this flow, producing a secondary perturbation. If this scenario causes a time delay in the chain relaxation, this delay should be proportional to the amplitude of the flow perturbation which, in turn, is proportional to the radius of the bead times its velocity before $t = 0$.

One of the practical difficulties in a quantitative theory of gel electrophoresis is the lack of information about the interaction between the charged DNA and the ionic media commonly used in gel electrophoresis. The relaxation experiments described here, however, depend almost exclusively on the elasticity of DNA and on the hydrodynamic properties of DNA and the gel. The reasonable agreement of the theory with experiments in pure solvent suggests that relaxation experiments in agarose gels are a good way to characterize the gels by their hydrodynamic shielding length. Then the present relaxation theory may be combined with that of electrophoretic stretch to treat the sliding of U-shaped DNA around a gel fiber in gel electrophoresis. Such a more general theory, presently under study, can be compared with the unhooking dynamics of DNA in a gel, as reported by Song and Maestre[3] and, for long DNA, by Gurrieri et al.[4]

It should be emphasized that the uniformly porous gel model developed in this paper, is useful only to treat the velocity of DNA in the various phases of its progress during gel electrophoresis. A (statistical) treatment of the path of DNA requires a quite different approach, based on the contact interactions between DNA and the gel. Here the gel may be modeled as a collection of obstructions, e.g. along the lines of Zimm's "lakes-straights" model.[25]

8. Conclusions

The stretching and relaxation of DNA during gel electrophoresis introduces long-range hydrodynamic interactions between remote segments of the DNA chain. The damping of this long-range interaction by an uncharged gel is treated by modeling the gel as a uniformly porous medium, and the segmented DNA as a succession of solid spheres. Relaxation of stretched DNA and electrophoretic stretch of DNA are formulated in terms of the hydrodynamic shielding length of the gel, using the entropic elasticity of DNA as treated by Marko and Siggia[10] and Zimm.[11]

The theory predicts that, at the critical trapping field strength, the total tether force at the gel contact is independent of the symmetry and of the size of the arrested DNA. This result suggests further experiments to illuminate the mechanism of trapping. Relaxation of the extension and of the tether force of stretched DNA in liquid scales with the contour length L_c approximately as $L_c^{1.70}$ and $L_c^{1.82}$ respectively, with somewhat higher exponents for relaxation in a gel. Relaxation experiments look promising for characterizing uncharged gels by their shielding length, a suitable parameter for quantitatively treating successive stages of gel electrophoresis.

Acknowledgment. Particular thanks are due to Prof. Stuart A. Allison for checking the mathematics of Appendix A. The author also thanks Dr. Douglas E. Smith for the experimental data in Figures 12−14.

Appendix A. Sphere Moving through Porous Medium

We consider a solid sphere with radius a moving with velocity v_0 along the z axis through a homogeneous porous medium with shielding length L and viscosity η. The liquid velocity u vanishes at infinity and must satisfy eqs 2 and 3, which we rewrite

$$\Delta u - u/L^2 - \nabla p/\eta = 0 \qquad \text{(A1)}$$

$$\nabla . u = 0 \qquad \text{(A2)}$$

Equation A1 is a set of three equations, one for each Cartesian coordinate. The solution below is a modification of that by Bueche[26] for the resistance of a porous sphere moving through a liquid medium. Taking the divergence of the terms in eq A1 yields the Laplace eq for p

$$\Delta p = 0 \tag{A3}$$

with the solution

$$p = B\frac{\partial}{\partial z}\left(\frac{1}{r}\right) \tag{A4}$$

where B is a constant.

We separate the liquid velocity into two parts $u = u_1 + u_2$. Here u_1 is the irrotational part of u, derivable from a velocity potential A with

$$u_1 = \nabla A \tag{A5}$$

and compensating the pressure distribution in eq A1. So A must satisfy

$$\Delta\nabla A - \nabla A/L^2 - \nabla p/\eta = 0 \tag{A6}$$

or

$$\Delta A - A/L^2 - p/\eta = 0 \tag{A7}$$

A solution is obtained by adding functions A_1 and A_2 which satisfy $-A_1/L^2 - p/\eta = 0$ with $\Delta A_1 = 0$, and $\Delta A_2 - A_2/L^2 = 0$. Such a solution, with $A(r = \infty) = 0$, is

$$A = -\frac{BL^2}{\eta}\frac{\partial}{\partial z}\left(\frac{1}{r}\right) + C\frac{\partial}{\partial z}\left(\frac{e^{-r/L}}{r}\right) \tag{A8}$$

in which the constants B and C are determined later from the boundary conditions at $r = a$.

In view of eqs A1 and A2 the second part u_2 of u must satisfy

$$\Delta u_2 - u_2/L^2 = 0 \tag{A9}$$

$$\nabla u_2 = -\nabla u_1 \tag{A10}$$

Such a solution is $(u_2)_x = 0$, $(u_2)_y = 0$, $(u_2)_z = -Ce^{-r/L}/L^2r$. With $u = \nabla A + u_2$ we obtain with eq A8

$$\begin{aligned} u_x &= -\frac{BL^2}{\eta}\frac{\partial^2}{\partial x\partial z}\left(\frac{1}{r}\right) + C\frac{\partial^2}{\partial x\partial z}\left(\frac{e^{-r/L}}{r}\right) \\ u_y &= -\frac{BL^2}{\eta}\frac{\partial^2}{\partial y\partial z}\left(\frac{1}{r}\right) + C\frac{\partial^2}{\partial y\partial z}\left(\frac{e^{-r/L}}{r}\right) \\ u_z &= -\frac{BL^2}{\eta}\frac{\partial^2}{\partial z^2}\left(\frac{1}{r}\right) + C\frac{\partial^2}{\partial z^2}\left(\frac{e^{-r/L}}{r}\right) - \frac{C}{L^2}\frac{e^{-r/L}}{r} \end{aligned} \tag{A11}$$

Completing the differentiations eq A11 becomes more explicitly

$$\begin{aligned} u_x &= -\frac{BL^2}{\eta}\frac{3xz}{r^5} + C\frac{xz}{r^5}e^{-r/L}\left(3 + \frac{3r}{L} + \frac{r^2}{L^2}\right) \\ u_y &= -\frac{BL^2}{\eta}\frac{3yz}{r^5} + C\frac{yz}{r^5}e^{-r/L}\left(3 + \frac{3r}{L} + \frac{r^2}{L^2}\right) \\ u_z &= -\frac{BL^2}{\eta}\frac{3z^2 - r^2}{r^5} + \\ &\quad C\frac{e^{-r/L}}{r^5}\left[3z^2 - r^2 + \frac{r}{L}(3z^2 - r^2) + \frac{z^2r^2}{L^2} - \frac{r^4}{L^2}\right] \end{aligned} \tag{A12}$$

From the velocity v_0 of the sphere, the boundary conditions at $r = a$

$$\begin{aligned} u_x &= 0 \\ u_y &= 0 \\ u_z &= v_0 \end{aligned} \tag{A13}$$

give the constants B and C

$$B = -\frac{1}{2}\eta a v_0\left(3 + 3\frac{a}{L} + \frac{a^2}{L^2}\right) \tag{A14}$$

$$C = -\frac{3}{2}aL^2e^{a/L}v_0 \tag{A15}$$

Substituting for B and C in the expression for u_z in eq A12, and using $z/r = \cos\theta$, gives eq 6 of the main text. In spherical coordinates the velocity components are, with eq A12 and $x/r = \sin\theta$,

$$u_r = u_z\cos\theta + u_x\sin\theta = \left[\frac{aL^2}{r^3}\left(3 + \frac{3a}{L} + \frac{a^2}{L^2}\right) - \frac{3aL^2}{r^3}\left(1 + \frac{r}{L}\right)e^{-(r-a)/L}\right]v_0\cos\theta \tag{A16}$$

$$u_\theta = -u_z\sin\theta + u_x\cos\theta = \left[\frac{aL^2}{2r^3}\left(3 + \frac{3a}{L} + \frac{a^2}{L^2}\right) - \frac{3aL^2}{2r^3}\left(1 + \frac{r}{L} + \frac{r^2}{L^2}\right)e^{-(r-a)/L}\right]v_0\sin\theta \tag{A17}$$

Expansions for large L, that is low porosity, are

$$u_r = \left[\frac{3a}{2r} - \frac{a^3}{2r^3} - \frac{a}{2L}\left(2 + \frac{a}{r}\right)\left(1 - \frac{a}{r}\right)^2 + \frac{ar}{8L^2}\left(3 + \frac{a}{r}\right)\left(1 - \frac{a}{r}\right)^3 + O(1/L^3)\right]v_0\cos\theta \tag{A18}$$

$$u_\theta = \left[-\frac{3a}{4r} - \frac{a^3}{4r^3} + \frac{a}{4L}\left(4 + \frac{a}{r} + \frac{a^2}{r^2}\right)\left(1 - \frac{a}{r}\right) - \frac{ar}{16L^2}\left(9 + \frac{2a}{r} + \frac{a^2}{r^2}\right)\left(1 - \frac{a}{r}\right)^2 + O(1/L^3)\right]v_0\sin\theta \tag{A19}$$

The force exerted by the liquid on the sphere is[14]

$$F = \int_0^\pi\left[\left(-p + 2\eta\frac{\partial u_r}{\partial r}\right)\cos\theta + \left(-\eta\frac{\partial u_\theta}{\partial r} + \frac{\eta}{r}u_\theta - \frac{\eta}{r}\frac{\partial u_r}{\partial\theta}\right)\sin\theta\right]_{r=a}2\pi a^2\sin\theta\,d\theta \tag{A20}$$

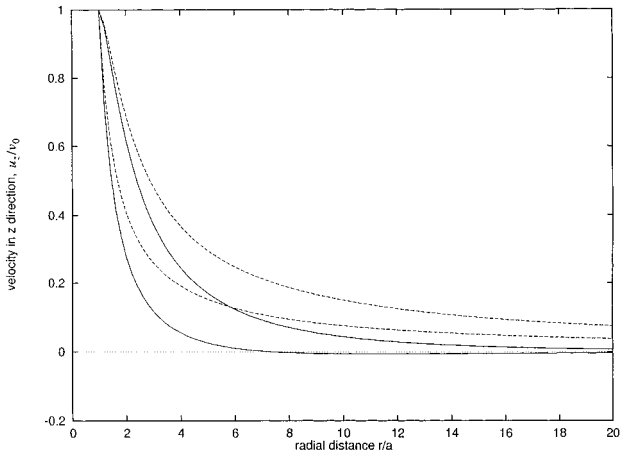

Figure 16. Relative liquid velocity in z direction around solid sphere moving with velocity v_0 along z axis. Solid curves: In gel with $L = 4 \times 10^{-8}$ m. Dashed curves: In pure liquid. Upper curves: In front or behind solid sphere, $\cos^2\theta = 1$ in eq 6. Lower curves: Next to sphere, $\cos\theta = 0$ in eq 6.

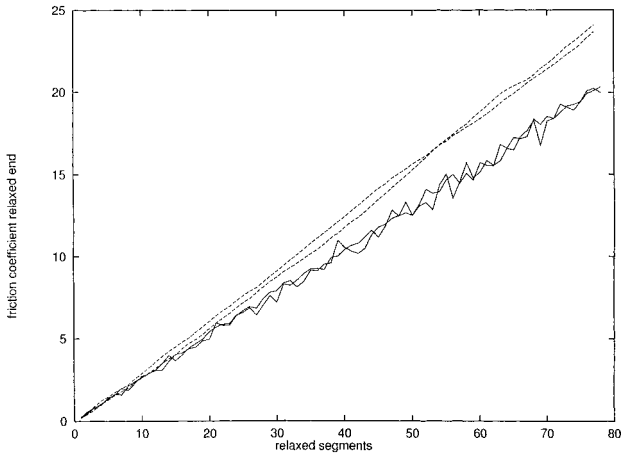

Figure 17. Hydrodynamic friction coefficient of fully relaxed end of chain with $N = 100$ segments in gel with $L = 4 \times 10^{-8}$ m for two different random number sequences. Solid curves: From theory with diffusion. Dashed curves: From theory without diffusion.

After integrating in eq A20 we obtain

$$F = -6\pi\eta a v_0\left(1 + \frac{a}{L} + \frac{a^2}{9L^2}\right) \qquad \text{(A21)}$$

giving eq 5 of the main text for the friction coefficient of the sphere in the porous medium. For $L = \infty$ we recover from eqs A18, A19, and A21 the Stokes results for the sphere moving through a viscous liquid.[14]

Figure 16 shows the relative velocity in the z direction, u_z/v_0, as a function of r/a, the radial distance in units of the sphere radius, as computed with eq 6. The dashed curves are for the sphere moving in pure liquid, the solid curves for moving in a porous medium with $L/a = 4$, corresponding approximately to a Kuhn segment of DNA moving through an agarose gel. In both media the upper curve is the liquid velocity in front and behind the sphere where $\cos^2\theta = 1$. The lower curves give the velocity for $\cos\theta = 0$, next to the sphere. As expected, in the porous medium the liquid motion is found to decay much faster than in pure liquid. The lower solid curve shows that in the porous medium, starting near $r/a = 8$, there is also a backflow, qualitatively as if the sphere were moving through a closed tube.

Appendix B. Hydrodynamic Resistance of Relaxed Part of Chain

For hydrodynamic purposes, the chain is represented by a collection of solid spheres. Here we compare the hydrodynamic resistance of the relaxed part of the chain in the theory with and without diffusion. Without diffusion the relaxed chain end has a flat configuration as in Figure 8, with diffusion it is three-dimensional as in Figure 5. For a chain of $N = 100$ segments, relaxing in a porous medium with $L = 4 \times 10^{-8}$ m, Figure 17 shows the friction coefficient of the fully relaxed part of $N - i_0$ segments for two different random number sequences. The solid curves are for the theory with diffusion, the dashed curves without diffusion. We find that, consistent with Figure 7, diffusion decreases the hydrodynamic resistance of the chain. The main reason is given in Figure 16 which shows that the flow behind or in front of a moving sphere is stronger than the flow next to it. For this reason the three-dimensional collection of spheres has more interaction and, hence, a smaller hydrodynamic resistance than the two-dimensional collection, irrespective of the somewhat different distance statistics among the spheres.

References and Notes

(1) Stellwagen, N. C. *Biopolymers* **1985**, *24*, 2243−2255.
(2) Smith, S. B.; Aldridge, P. K.; Callis, J. B. *Science* **1989**, *243*, 203−206.
(3) Song, L.; Maestre, M. F. J. *Biomol. Struct. Dyn.* **1991**, *9*, 87−99.
(4) Gurrieri, S.; Smith, S. B.; Bustamante, C. *Proc. Natl. Acad. Sci. U.S.A.* **1999**, *96*, 453−458.
(5) Burlatsky, S.; Deutch, J. *Science* **1993**, *260*, 1732−1734; *264*, 113.
(6) Viovy, J. L.; Duke, T. *Science* **1994**, *264*, 112−113.
(7) Stigter, D.; Bustamante, C. *Biophys. J.* **1998**, *75*, 1197−1210.
(8) Hunter, R. J. *Zeta Potential in Colloid Science*; Academic Press: New York, 1981.
(9) Debye, P.; Bueche, A. M. *J. Chem. Phys.* **1948**, *16*, 573−579.
(10) Marko, J. F.; Siggia, E. D. *Macromolecules* **1995**, *28*, 8759−8770.
(11) Zimm, B. H. *Macromolecules* **1998**, *31*, 6089−6098.
(12) Wiersema, P. H. Ph.D. Thesis, Utrecht, 1964.
(13) Stigter, D. *J. Phys. Chem.* **1980**, *84*, 2758−2762.
(14) Landau, L. D.; Lifshitz, E. M. *Fluid Mechanics*; Pergamon: New York, 1958.
(15) Oberbeck, A. *Crelles J.* **1876**, *81*, 62−80.
(16) Happel, J.; Brenner, H. *Low Reynolds Number Hydrodynamics*; Prentice Hall, Englewood Cliffs, NJ, 1965.
(17) Stellwagen, N. C.; Gelfi, C.; Righetti, P. G. *Biopolymers* **1997**, *42*, 687−703.
(18) Stigter, D. *J. Phys. Chem.* **1978**, *82*, 1417−1423; 1424−1429.
(19) Stigter, D. *Biopolymers* **1991**, *31*, 169−176.
(20) Adamson, A. W. *Physical chemistry of surfaces*; Interscience: New York, 1960.
(21) Smith, S. B.; Cui, Y.; Bustamante, C. *Science* **1996**, *271*, 795−798.
(22) Perkins, T. T.; Quake, S. R.; Smith, D. E.; Chu, S. *Science* **1994**, *264*, 822−826.
(23) Smith, S. B.; Finzi, L.; Bustamante, C. *Science* **1992**, *258*, 1122−1126.
(24) Zimm, B. H. *J. Chem. Phys.* **1956**, *24*, 269−278.
(25) Zimm, B. H. *J. Chem Phys.* **1991**, *94*, 2187−2206.
(26) Bueche, A. M. 1951. Private communication.

MA0009350